

The Study of Electrical Grid Components After Installing a 10 MW Photovoltaic Power Plant with Large-Scale Batteries at Peak Load by DigSilent Software

Mohammad Parhamfar^{1,*}, Amir Mohammad Adeli²

¹Business Management, MSc in Renewable Energy, Electrical and Energy Industry Advisor, Isfahan, Iran

²Planning and Management of Electrical Energy Systems, Shahid Beheshti University, Tehran, Iran

Email address:

info@parhamfar.com (Mohammad Parhamfar), amir.adeli4428@gmail.com (Amir Mohammad Adeli)

*Corresponding author

To cite this article:

Mohammad Parhamfar, Amir Mohammad Adeli. The Study of Electrical Grid Components After Installing a 10 MW Photovoltaic Power Plant with Large-Scale Batteries at Peak Load by DigSilent Software. *American Journal of Electrical Power and Energy Systems*. Vol. 11, No. 5, 2022, pp. 97-107. doi: 10.11648/j.epes.20221105.12

Received: September 15, 2022; **Accepted:** October 18, 2022; **Published:** October 27, 2022

Abstract: Taking into mind the plans and feasible targets for installing renewable power plants, particularly solar farms in Iran, and the fact that the energy generated by these power plants during the day and at different periods of the year is variable, sudden events such as a fall or increase in demand, as well as changes in grid components, should be taken into account when evaluating these power plants. Controlling the slope of the duck curve and grid components will rely heavily on energy storage. As a result, one of the most recent options proposed by top corporations is the use of large-scale batteries. The increase in peak load is one of the issues that will develop in Iran in the future. Given the abundance of 10 MW solar power plants in Iran, this article attempts to demonstrate the effect of installing a large-scale battery in a 10 MW photovoltaic power plant on power grid performance By DigSilent software. Finally, the grid's power quality components are examined. The effect of installing a large-scale battery in a 10 MW photovoltaic power plant on power grid performance was explored in this article utilizing DigSilent software. Some parameters such as Maximum power generation of the plant with storage, AC Loss, Maximum power injection with storage, Operation coefficient of the upstream station, and Voltage of the 20kv bus of the upstream station, have been calculated.

Keywords: Renewable Energy, Duck Curve, DigSilent Software, Power Quality, Battery

1. Introduction

Electricity demand is increasing on the global market. Figure 1 depicts global electricity usage by region from 1990 to 2017. During this time, electricity demand climbed by 72%, with an annual growth rate of 4% on average. At the end of 2017, global electricity demand exceeded 23,000 TWh. China and other developing countries are experiencing the fastest growth in electricity demand. This is due to the advancement of industrialization, which has increased human comfort and population [1]. With increased electricity demand, fossil fuels are depleted to the point where they may not last more than a few decades. Furthermore, the cost of

petroleum products is rising. As a result, the global demand for renewable energy as a viable alternative to fossil fuels is expanding fast [2].

However, because renewable energy production is dependent on external elements such as wind speed, solar radiation, and water flow intensity, their energy generation schedule cannot be regulated, and their efficiency and flexibility are diminished [3]. The adoption of energy storage systems can greatly minimize these constraints. Batteries, flow cells (flow batteries), and supercapacitors are all choices for storing energy generated by renewable energy sources. Supercapacitors outperform regular capacitors and secondary ion batteries [4].

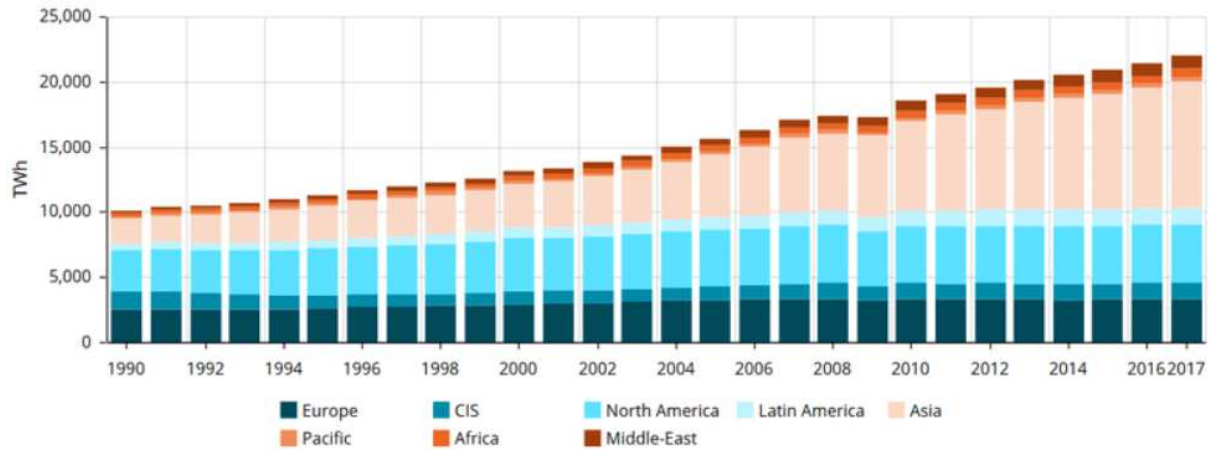


Figure 1. Global energy consumption by region from 1990 to 2017 (Global Energy Statistical Yearbook, 2018).

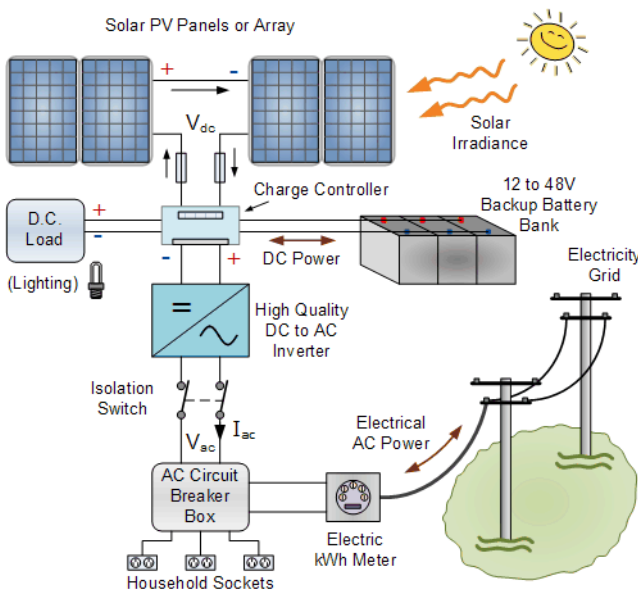


Figure 2. A Conventional PV system with battery.

We have seen a rapid advancement in technology over the last decade with the goal of developing new technologies for converting solar photovoltaic energy into electricity and storing it electrochemically utilizing devices such as batteries. The next step in this path is to integrate photovoltaic energy conversion systems and energy storage systems. An activity that necessitates significant advancements in electronic equipment engineering, energy management, and metallurgy [5].

The integration of solar photovoltaic energy conversion systems and batteries is critical to achieve the major goals of decreasing generation fluctuations, lowering reliance on fossil fuels, addressing the issue of carbon dioxide emissions, and so on [6]. The deployment of solar systems and battery installation has increased rapidly in recent years. Due to the vast number of characteristics that might affect utility stability, the optimal use of photovoltaic and battery systems is a critical issue for designers, users, and network operators [7].

2. A Review on Photovoltaic System and Battery Management

Photovoltaic systems were first used to power spacecrafts and satellites in 1958, and they have since found numerous applications [8]. Water pumping [9, 10], hydrogen generation [11, 12], and, most critically, electricity provision to rural communities and villages are the primary applications of these systems [8]. Figure 2 depicts a photovoltaic system built for this purpose. This system is made up of solar panels, batteries, loads, DC/DC converters, and inverters. The size of solar panels and battery capacity are determined by load demand, environmental and economic conditions, and other factors. During the day, the solar panel turns the sun's photon energy into electricity, which can be supplied periodically and stored in the battery for later use. Furthermore, excess electricity from photovoltaic systems connected to the grid can be pumped into the grid to supply power. Photovoltaic power plants contain a battery management system and a load management system to optimize energy storage and utilization.

The battery management system is a real-time system that is important to safe and efficient operation of the battery system. A typical battery management system is made up of sensors, actuators, and microcontrollers that perform the following tasks:

- 1) Data acquisition: voltage, current, and temperature signals are sampled and converted to digital signals before being supplied to the control unit as input to the battery management algorithms.
- 2) Status estimation: Accurate battery status estimation is essential for further managing the battery system. In addition to the battery's state of health (SOH), the significant states that must be estimated include the battery's state of charge (SOC) [13], the battery's state of power (SOP) [14], and so on.
- 3) Fault detection: is conducted to protect the safety and functioning of the battery bank; its main tasks include short circuit detection and warning, excessive

charge/discharge, sensor/actuator error, and so on [15].

- 4) Cell balance: Cell balance's goal is to enhance the performance of the battery bank, which is made up of parallel and series cells [16].
- 5) Thermal management: The thermal management unit maintains the temperature of the battery bank to ensure that the batteries operate safely and efficiently [17].

3. Problem's Objective

The main objective of this study is to model and investigate the effect of 10Mw solar power plant with energy storage systems on electrical parameters of the utility.

4. Problem Assumptions

- 1) During the winter (low load), the upstream station's load equals 40% of the peak period's load.
- 2) Given the total generation of the plant and the storage during summer (peak period) and assuming 80% operation capacity for the transformer, the capacity of the 0.4 to 20Kv transformers is selected to be 2.5 MvA.

Given that the output voltage of the storage devices is of the DC type, the storage devices are linked to the DC bus of the solar panels as shown in single line diagram of Figure 3. As you can see, eight storages are connected to eight DC buses of solar panels.

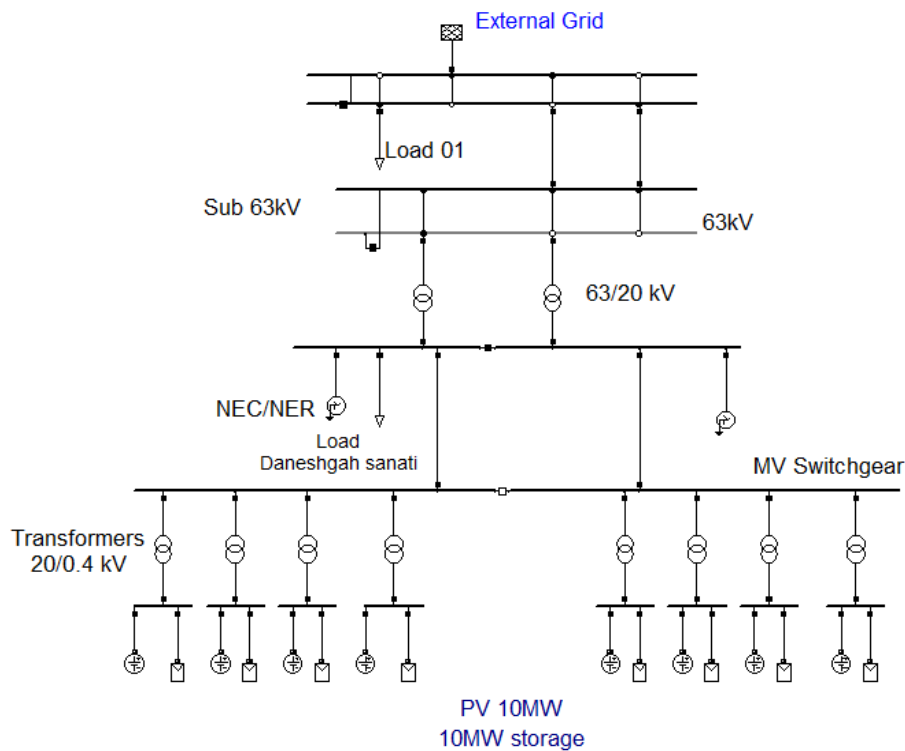


Figure 3. Single line diagram of the power plant and connection to the upstream station in DigSilent.

It is required to mention that the solar power plant with a capacity of 10 MW was first modeled in the PVsyst software in the examined geographical region. The hourly output of the solar power plant for one year is presented in Table 1.

Table 1. Hourly generation of the solar plant for one year.

Hourly	Monthly											
	January	February	March	April	May	June	July	August	Septemb	October	Novemb	Decemb
	E_Grid [MW]	E_Grid [MW]	E_Grid [MW]	E_Grid [MW]	E_Grid [MW]	E_Grid [MW]	E_Grid [MW]	E_Grid [MW]	E_Grid [MW]	E_Grid [MW]	E_Grid [MW]	E_Grid [MW]
0H	0	0	0	0	0	0	0	0	0	0	0	0
1H	0	0	0	0	0	0	0	0	0	0	0	0
2H	0	0	0	0	0	0	0	0	0	0	0	0
3H	0	0	0	0	0	0	0	0	0	0	0	0
4H	0	0	0	0	0	0	0	0	0	0	0	0
5H	0	0	0	0	0.1	0.2	0.1	0	0	0	0	0
6H	0	0	0.1	0.9	1.4	1.6	1.3	1.2	0.8	0.3	0	0
7H	0.3	1.1	1.6	2.9	3.3	3.5	3.1	3.3	2.8	2.4	1.5	0.7
8H	2.6	3.1	3.6	4.7	5.2	5.4	4.9	8.3	4.8	4.5	3.4	2.7
9H	4.6	4.9	5.1	6	6.7	6.8	6.3	7	6.3	6	4.8	4.3
10H	5.8	6.2	6.3	7	7.7	7.9	7.4	8.1	7.4	7.1	5.8	5.3
11H	6.2	6.9	6.3	7.2	8.2	8.4	7.6	8.3	7.8	7.2	6.2	5.8

Hourly	Monthly											
	January	February	March	April	May	June	July	August	Septemb	October	Novemb	Decemb
	E Grid	E Grid	E Grid	E Grid	E Grid	E Grid	E Grid	E Grid	E Grid	E Grid	E Grid	E Grid
	[MW]	[MW]	[MW]	[MW]	[MW]	[MW]	[MW]	[MW]	[MW]	[MW]	[MW]	[MW]
12H	6.1	7.1	6.3	7.2	8.1	8.3	7.5	8.3	7.8	7	6.2	5.7
13H	5.4	6.9	5.7	6.5	7.5	7.7	7.1	7.8	7.1	6.4	5.4	5.3
14H	4.3	5.8	4.8	5.5	6.4	6.6	6.2	6.7	5.9	5.1	4.1	4
15H	2.8	4.1	3.7	4	4.8	5.1	4.8	5.1	4.2	3.3	2.3	2.1
16H	0.8	1.9	2	2.3	2.9	3.2	3.1	3.2	2.2	1.2	0.2	0.1
17H	0	0	0.4	0.7	1.1	1.4	1.3	1.2	0.4	0	0	0
18H	0	0	0	0	0	0.1	0.1	0	0	0	0	0
19H	0	0	0	0	0	0	0	0	0	0	0	0
20H	0	0	0	0	0	0	0	0	0	0	0	0
21H	0	0	0	0	0	0	0	0	0	0	0	0
22H	0	0	0	0	0	0	0	0	0	0	0	0
23H	0	0	0	0	0	0	0	0	0	0	0	0

5. Problem Statement

According to the above table, the hourly generation curve of panels and the absorption-generation curve of storages must be modeled in software. The Time Characteristics feature in the software is utilized for this purpose. The following four time-curves are considered:

- 1) Daily hourly generation curve of the panel during the peak period, called Time Characteristic for PV-Peak- Figure 4.
- 2) Daily hourly generation curve of the panel during the low load period, called Time Characteristic for PV-Light- Figure 5.
- 3) Absorption-Generation curve of the storage during peak

period, called Time Characteristic for Storage-Peak- Figure 6.

- 4) Absorption-Generation curve of the storage during low load period, called Time characteristic for Storage-Light- Figure 7.

Figure 4 shows June of Table 1, modeled in DigSilent and represents the output energy generation of the power plant in DigSilent.

Such that in Figure 4, the step curve of the total daily hourly generation of the solar power plant in June is shown, and the horizontal curve shows the start and end hours of the steps of the solar power plant generation in a summer day, and the vertical curve shows the total energy (MWh) injection at different times of the day.

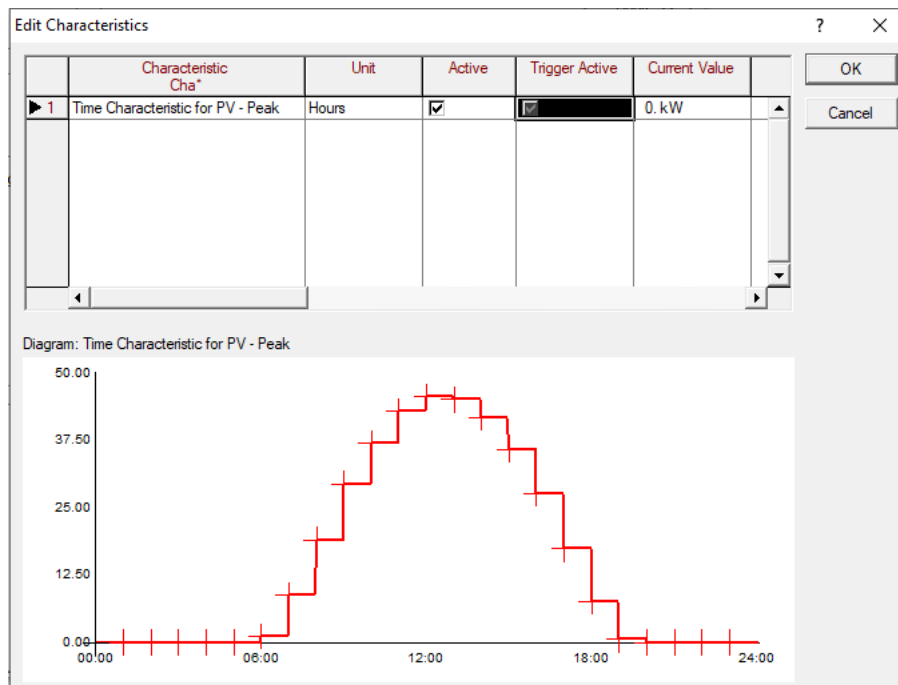


Figure 4. Daily hourly generation curve of the panels during the peak period.

For example, at 10 a.m., the solar power plant generates approximately 6.2 megawatts, which is considered to be 17.5MWh for modeling the energy representation, and according to the items presented in table 1, the total energy

generated by the solar power plant until 10 a.m. is estimated to be 17.5 MWh in June.

In Figure 5, the step curve of the total daily hourly generation of the solar power plant in January, according to

Table 1, is shown, and the horizontal curve shows the start and end hours of the steps of the solar power plant generation

in a January day, and the vertical curve shows the total energy (MWh) injection at different times of the day.

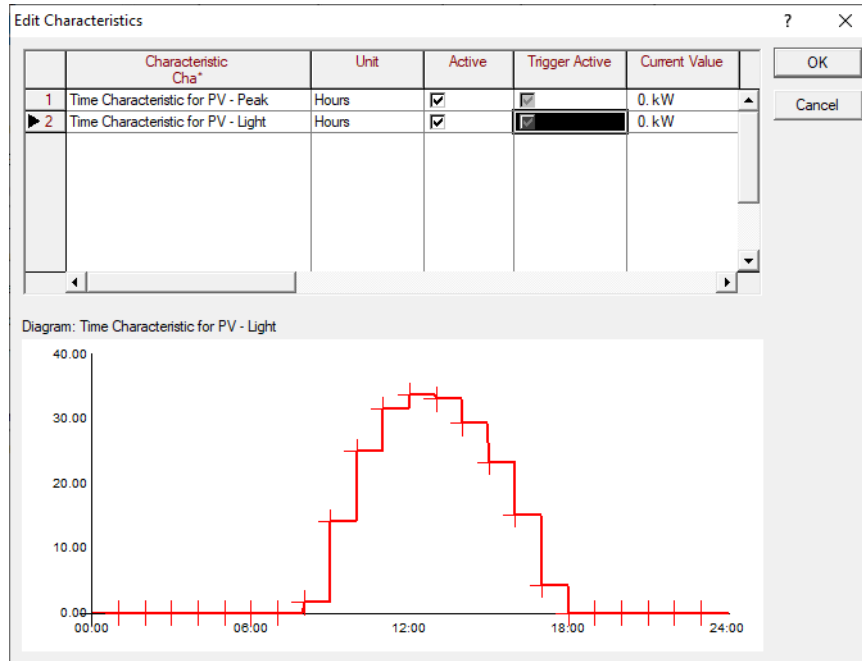


Figure 5. Daily hourly generation curve of the panels during low load period.

For example, at 9 a.m., the solar power plant generates roughly 4.6 MW, which is considered to be 7.5MWh for modeling the energy representation, and according to the items presented in table 1, the total energy generated by the solar power plant until 9 a.m. is estimated to be 7.5 MWh in June.

the storage (absorption curve) during one summer day after modeling the storage with DigSilent program. So, because the peak time in summer in this model is between 13:00 and 17:00, the solar power plant absorbs energy in the storage device until 13:00, at which point the storage device is activated and the energy delivered by the power plant is injected to the grid.

Figure 5 depicts the connection and disconnection curves of

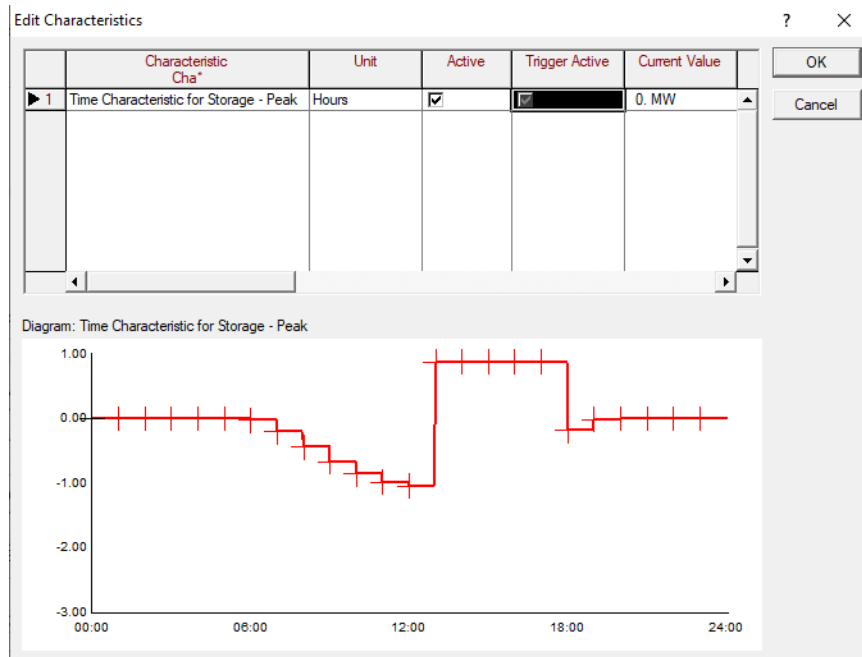


Figure 6. Absorption-Generation Curve of the Storage in the peak period.

Figure 6 depicts the storage connection and disconnection curve (absorption curve) for a single winter day. Thus, the

peak period in winter is between 13:00 and 18:00, and the peak time at night is between 20:00 and 21:00, according to

this modeling. The solar power plant absorbs energy in the storage device until 13:00, at which point the storage device becomes operational, and the energy generated by the power plant is injected to the grid.

Because the solar power plant does not generate at night, the energy storage gradually injects the energy generated by

the plant during the day to the grid, and there will be no energy left for injection at night. It should be mentioned that depending on whether the power is required at the peak or at night, a storage can be configured to generate at night; therefore, in this study, the storage device should only be used during the peak hour and inject power to the grid.



Figure 7. Absorption-Generation curve of the storage at low-load period.

Using Quasi-Dynamic analysis in DigSilent, 24 power flows are taken and the following curves are obtained:

- 1) Hourly generation of a set of panels (23) in the peak and low load periods in Figures 8 and 9;
- 2) Injection power of the power plant and storage to the 20kV bus of the upstream station during low load and

- peak periods in Figures 10 and 11;
- 3) Voltage of 20 kV bus of the upstream station during peak and low load hours in Figures 12 and 13;
- 4) Upstream station's loading during low load and peak hours in Figures 14 and 15.

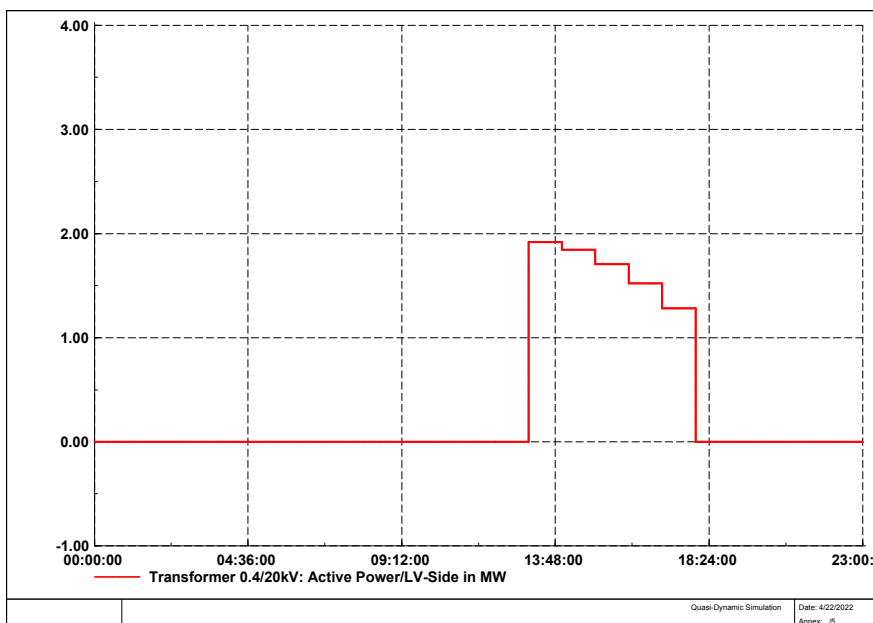


Figure 8. Hourly generation of one set of panels (23) during peak period.

Figures 8–18 depict hourly generation, injection power, bus voltage, and upstream station loading as the storage enters the circuit.

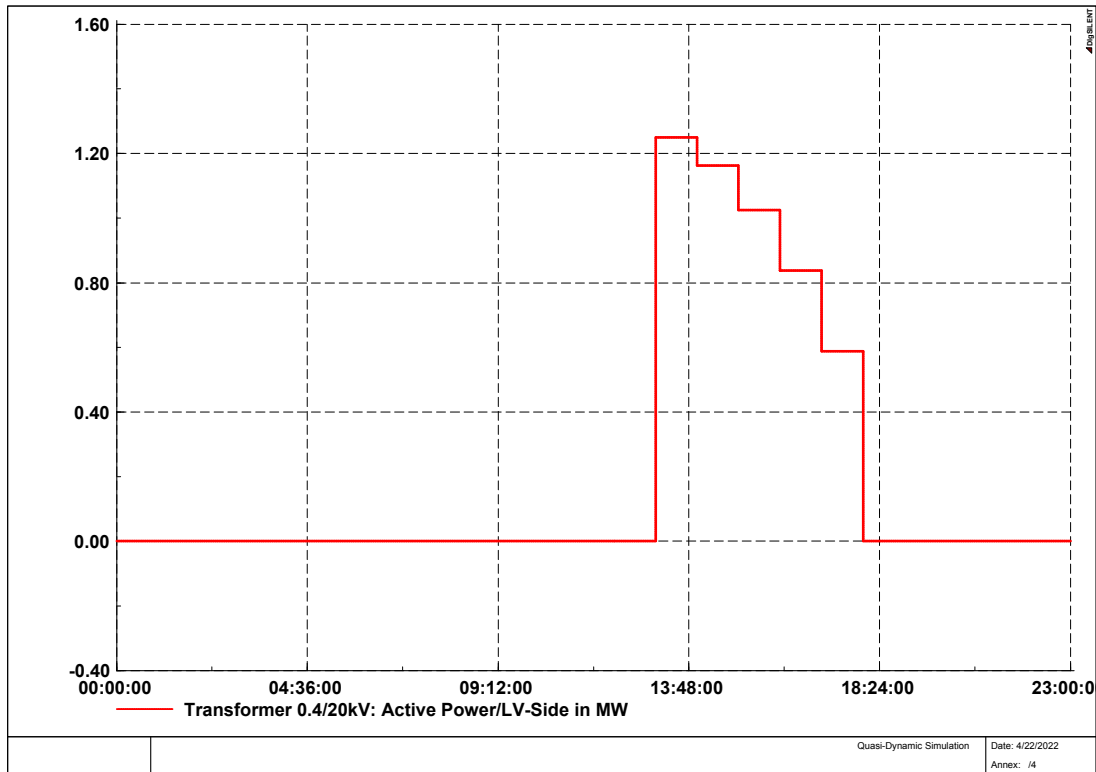


Figure 9. Hourly generation of a set of panels (23) during low load period.

According to the above figure, it is clear that the storage is controlled and managed by a battery management system so that it is connected to the circuit when required (peak time in this study) and deliver the stored energy to the grid.

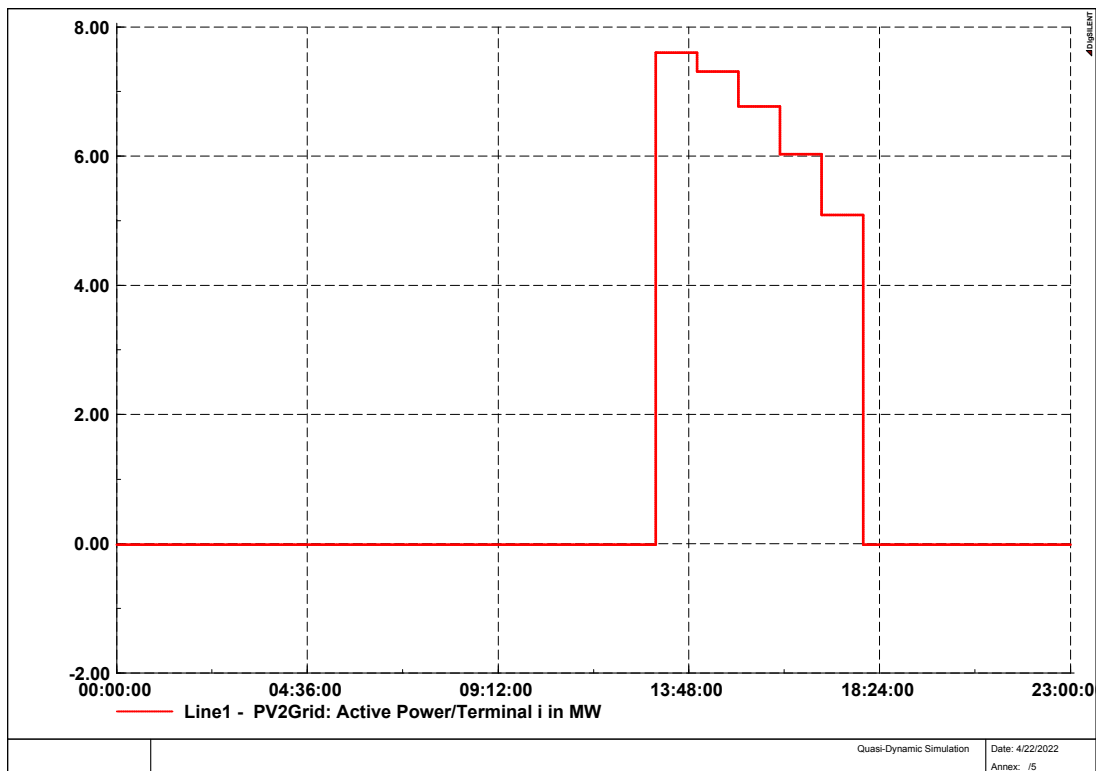


Figure 10. Power injection of the plant and the storage to the 20kV bus of the upstream station during the peak period.

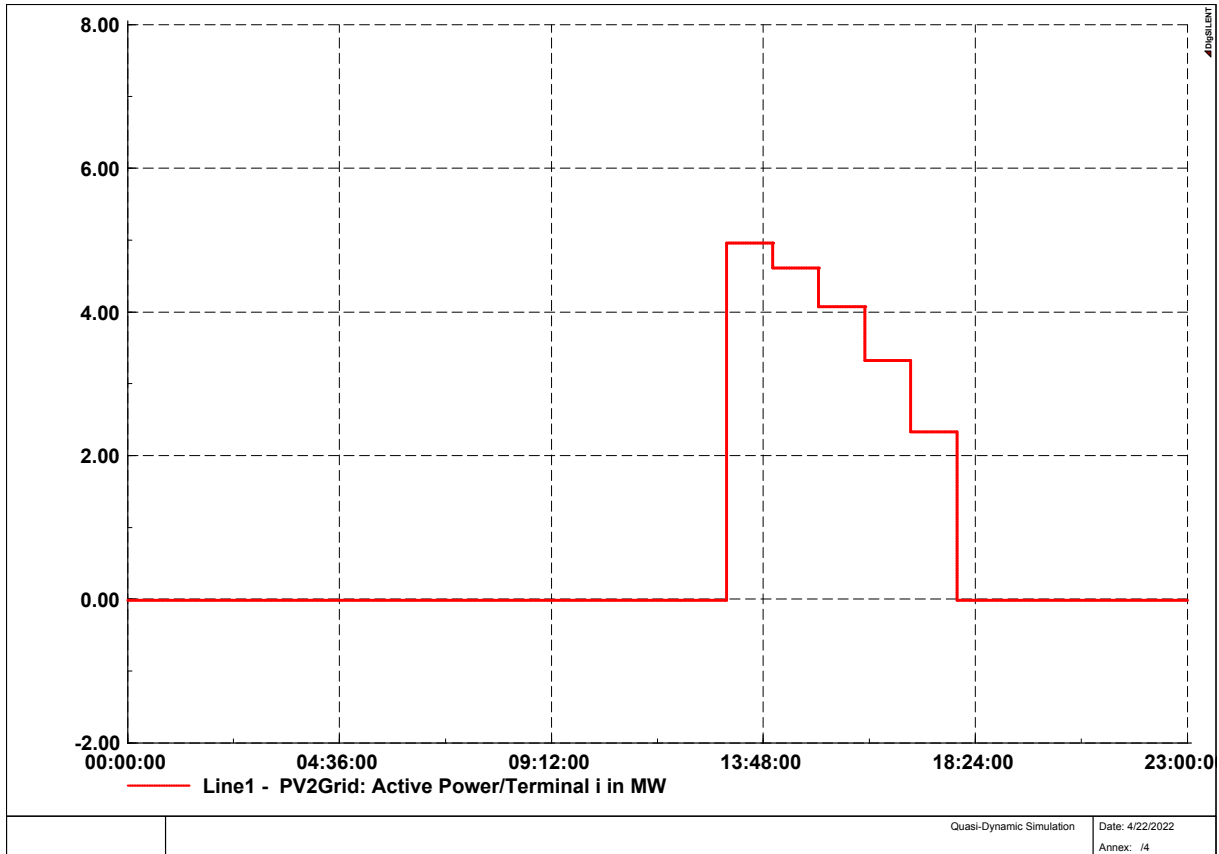


Figure 11. Power injection of the plant and the storage to the 20kV bus of the upstream station during the low load period.

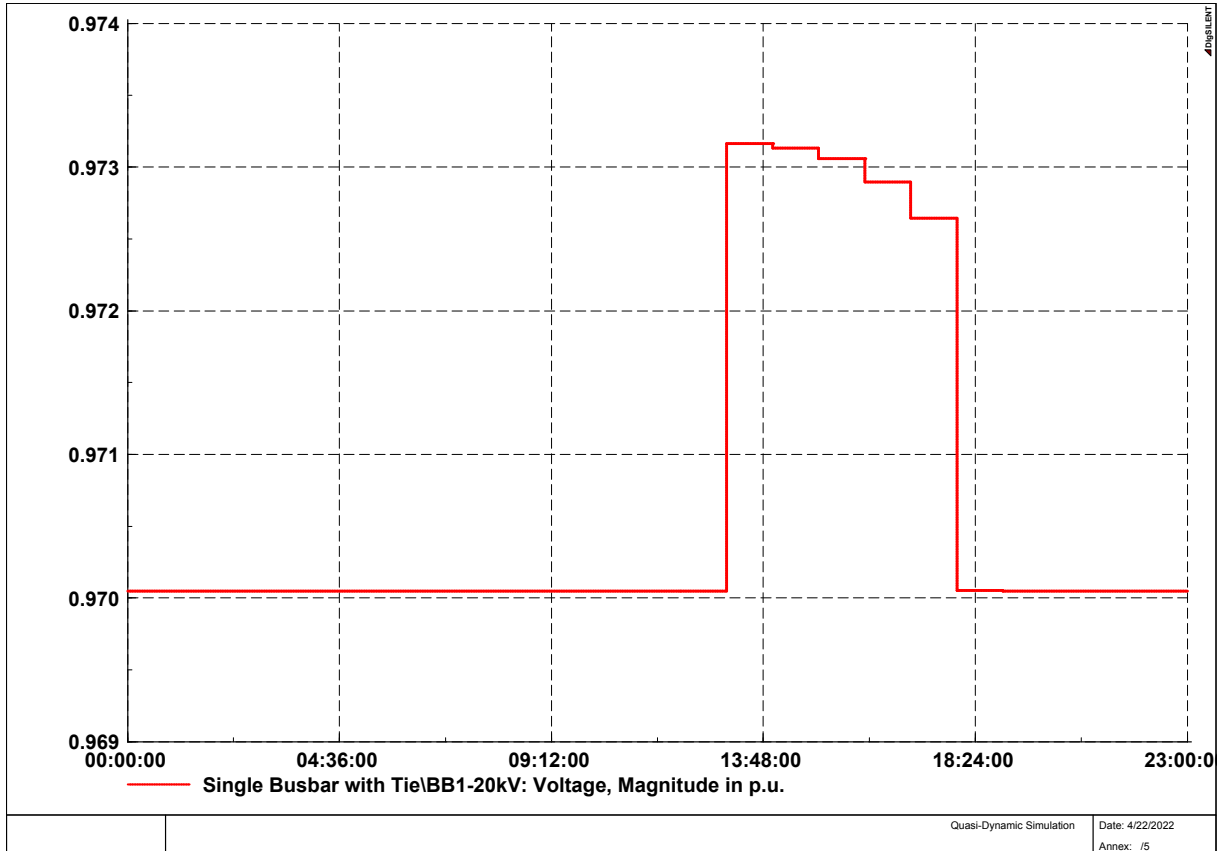


Figure 12. Voltage of the 20kV bus of the upstream station during the peak period.

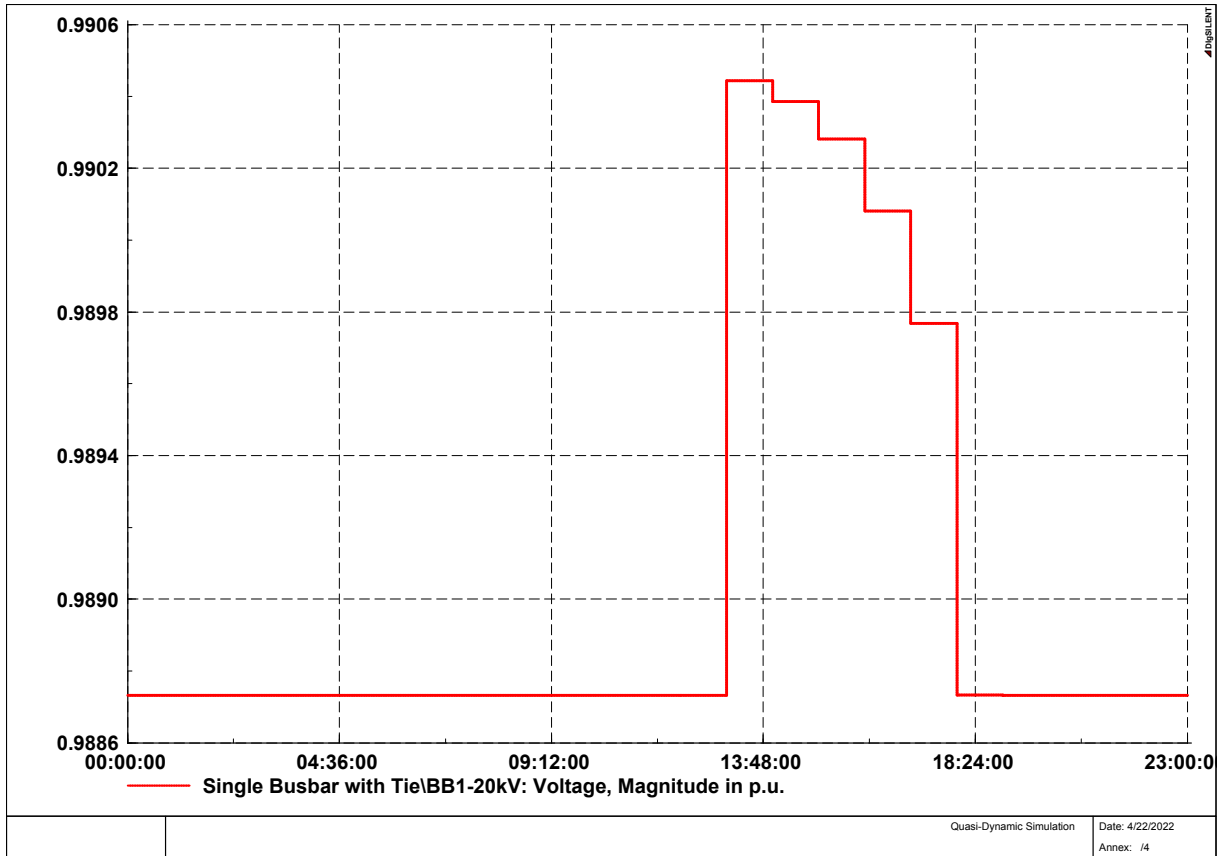


Figure 13. Voltage of the 20kV bus of the upstream station during the low load period.

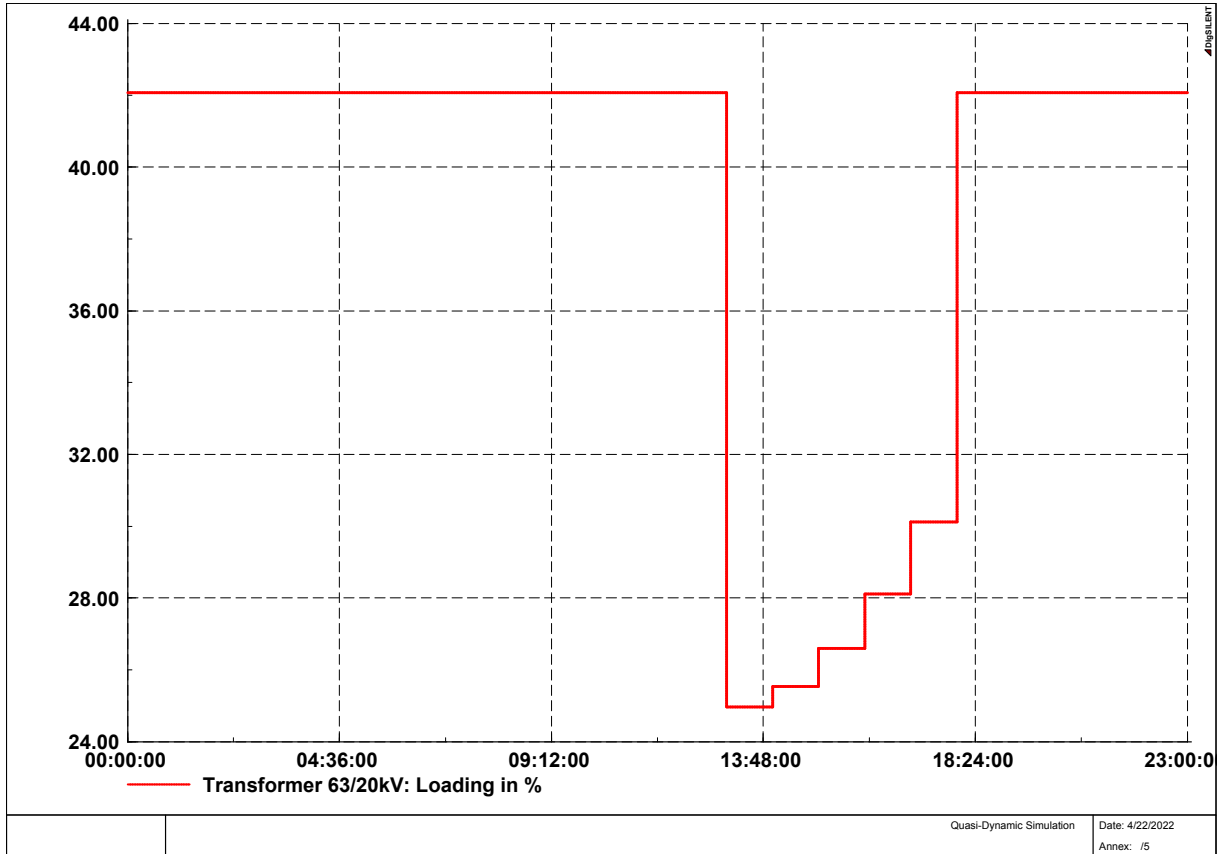


Figure 14. Loading of the upstream station during the peak period.

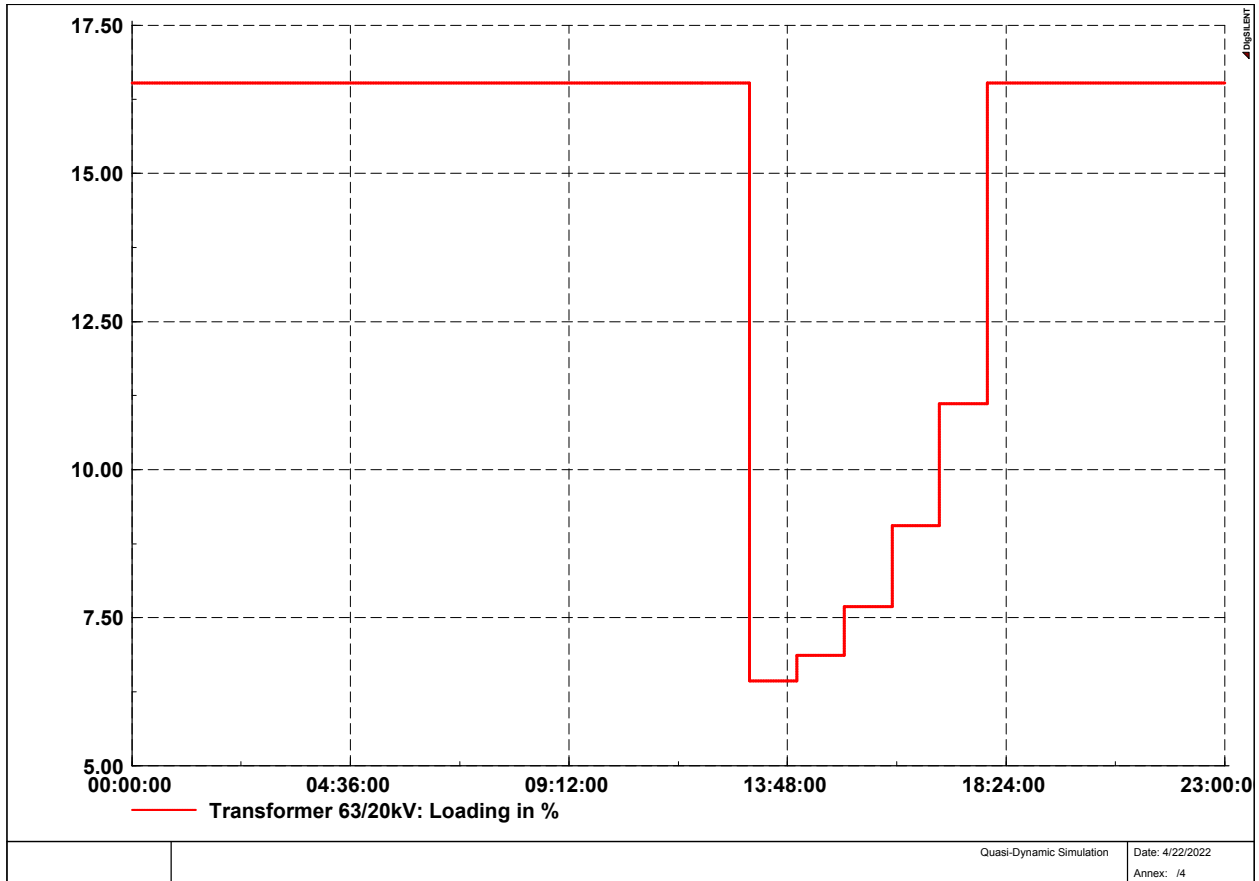


Figure 15. Loading of the upstream station during the low load period.

6. Conclusion

The effect of installing a large-scale battery in a 10 MW photovoltaic power plant on power grid performance was explored in this article utilizing DigSilent software. Because the solar power plant does not generate at night, the stored energy generated by the power plant during the day is gradually injected into the grid, and there will be no energy left for injection at night. It should be mentioned that depending on whether the power is required at the peak or at

night, the storage can be configured to generate at night; however, in this study, the storage should only be used during the peak and inject power to the grid. Important information of Figures 6-13 is summarized in Tables 2 and 3. As can be seen, by connecting the plant and the storage to the grid during peak and low load periods, a power equal to 14.962 and 9.82Mw is injected to the 20kV bus of the upstream station, which reduces loading of the upstream station to 17.1 and 10.09, and increases the voltage of the 20Kv bus of the upstream station to 0.003 and 0.001 p.u., and reduces loss of the upstream station to 30 and 6Kv.

Table 2. Power generation of the plant in summer and winter.

Parameter	Summer (peak load)	Winter (low load)
Maximum power generation of the plant with storage (MW)	15.36	10
AC Loss (MW)	0.398	0.18
Maximum power injection with storage (MW)	14.962	9.82

Table 3. Electrical parameters of the grid before and after connecting the plant and the storage to the grid.

Parameter	Summer (peak load)		Winter (low load)	
	Before connecting the plant with storage	After connecting the plant with storage	Before connecting the plant with storage	After connecting the plant with storage
Operation coefficient of the upstream station (percent)	42.07	24.97	16.53	6.44
Voltage of the 20kv bus of the upstream station	0.97	0.973	0.989	0.990
losses of the upstream station (kv)	47	17	7	1

References

- [1] International Energy Agency (2018).
- [2] M. Combe, A. Mahmoudi, M. H. Haque, R. Khezri; Cost effective sizing of an AC mini-grid hybrid power system for a remote area in South Australia; *IET Gener, Transm Distrib*, 13 (2) (2019), pp. 277-287.
- [3] Parhamfar, Mohammad; Adeli, Amir Mohammad; Mousavi, Shahin; Large-scale renewable energy storage systems: Review on the social benefits and services of entering the electricity market; The 6th National Conference of Electrical Engineering and Intelligent Systems; Islamic Azad University, Najaf-Abad Branch; June 2022.
- [4] Parhamfar, Mohammad; Adeli, Amir Mohammad; Mousavi, Shahin; An review on energy storage technologies and their integration with renewable energy sources in microgrids; The 6th National Conference of Electrical Engineering and Intelligent Systems; Islamic Azad University, Najaf-Abad Branch; June 2022.
- [5] Lucia Fagiolari, Matteo Sampò, Andrea Lamberti, Julia Amicia, Carlotta Francia, Silvia Bodoardo, Federico Bella; Integrated energy conversion and storage devices: Interfacing solar cells, batteries and supercapacitors; *Energy Storage Materials*; Volume 51, October 2022, Pages 400-434.
- [6] Yi Zhang, Hexu Sun, Jianxin Tan, Zheng Li, Weimin Hou, Yingjun Guo; Capacity configuration optimization of multi-energy system integrating wind turbine/photovoltaic/hydrogen/battery; *Energy*; Volume 252, 1 August 2022, 124046.
- [7] Rahmat Khezri, Amin Mahmoudi, Hirohisa Akib; Optimal planning of solar photovoltaic and battery storage systems for grid-connected residential sector: Review, challenges and new perspectives; *Renewable and Sustainable Energy Reviews*, Volume 153, January 2022, 111763.
- [8] El Chaar L, Lamont LA, El Zein N. Review of photovoltaic technologies. *Renew Sustain Energy Rev* 2011; 15: 2165e75. <https://doi.org/10.1016/j.rser.2011.01.004>.
- [9] Djoudi Gherbi A, Hadj Arab A, Salhi H. Improvement and validation of PV motor-pump model for PV pumping system performance analysis. *Sol Energy* 2017; 144: 310e20. <https://doi.org/10.1016/j.solener.2016.12.042>.
- [10] Tiwari AK, Kalamkar VR. Effects of total head and solar radiation on the performance of solar water pumping system. *Renew Energy* 2018; 118: 919e27. <https://doi.org/10.1016/j.renene.2017.11.004>.
- [11] Nguyen Duc T, Goshome K, Endo N, Maeda T. Optimization strategy for high efficiency 20 kW-class direct coupled photovoltaic-electrolyzer system based on experiment data. *Int J Hydrogen Energy* 2019; 44: 26741e52. <https://doi.org/10.1016/j.ijhydene.2019.07.056>.
- [12] Jafari M, Armaghan D, Seyed Mahmoudi SM, Chitsaz A. Thermoeconomic analysis of a standalone solar hydrogen system with hybrid energy storage. *Int J Hydrogen Energy* 2019; 44: 19614e27. <https://doi.org/10.1016/j.ijhydene.2019.05.195>.
- [13] Zheng Y, Ouyang M, Han X, Lu L, Li J. Investigating the error sources of the online state of charge estimation methods for lithium ion batteries in electric vehicles. *J Power Sources* 2018; 377: 161e88. <https://doi.org/10.1016/j.jpowsour.2017.11.094>.
- [14] Tang X, Wang Y, Yao K, He Z, Gao F. Model migration based battery power capability evaluation considering uncertainties of temperature and aging. *J Power Sources* 2019; 440: 227141. <https://doi.org/10.1016/j.jpowsour.2019.227141>.
- [15] Bhadra S, Hsieh AG, Wang MJ, Hertzberg BJ, Steingart DA. Anode characterization in zinc-manganese dioxide AA alkaline batteries using electrochemical-acoustic time-of-flight analysis. *J Electrochem Soc* 2016; 163: A1050e6. <https://doi.org/10.1149/2.1201606jes>.
- [16] Ling R, Wang L, Huang X, Dan Q, Zhang J. A review of equalization topologies for lithium-ion battery packs. *Chin Control Conf* 2015. <https://doi.org/10.1109/ChiCC.2015.7260899>. 2015eSept:792-2e7.
- [17] Ling Z, Zhang Z, Shi G, Fang X, Wang L, Gao X, et al. Review on thermal management systems using phase change materials for electronic components, Li-ion batteries and photovoltaic modules. *Renew Sustain Energy Rev* 2014; 31: 427e38. <https://doi.org/10.1016/j.rser.2013.12.017>.